

Anisotropic Reorientation of 9-Methylpurine and 7-Methylpurine Molecules in Methanol Solution Studied by Combining ^{13}C and ^{14}N Nuclear Spin Relaxation Data and Quantum Chemical Calculations

Dmytro Kotsyubynskyy and Adam Gryff-Keller*

Faculty of Chemistry, Warsaw University of Technology, Noakowskiego 3, 00-664 Warsaw, Poland

Received: October 20, 2006; In Final Form: December 8, 2006

Reorientation of 9-(trideuteromethyl)purine and 7-(trideuteromethyl)purine molecules in methanol- d_4 solutions has been investigated on the basis of the interpretation of the nuclear spin relaxation rates of their ^{14}N (or ^1H) and ^{13}C nuclei. The transverse quadrupole relaxation rates of ^{14}N nuclei have been obtained from the line shape analysis of their ^{14}N NMR spectra. Alternatively, the information on the longitudinal ^{14}N relaxation rates has been obtained via the scalar relaxation of the second kind of protons coupled to ^{14}N . The longitudinal dipolar relaxation rates of the protonated ^{13}C nuclei in the investigated molecules have been determined by measuring their overall relaxation rates and NOE enhancement factors. The molecular geometries, scalar coupling constants, and EFG tensors needed for quantitative interpretation of the above data have been calculated theoretically [DFT B3LYP/6-311++G(2d,p) or B3PW91/6-311+G(df,pd)] including the impact of the solvent by using discrete solvation and the polarizable continuum model. The reorientation of the investigated purines has been described as rotational diffusion of an asymmetrical top. It has been found that to get a fully consistent interpretation of the relaxation data, effective C–H bond lengths being 3% longer than the calculated ones had to be used in analysis to compensate for the ground-state vibrations. The obtained rotational diffusion coefficients and orientations of the principal diffusion axes show that the investigated molecules reorient anisotropically and that the mode of their solvation is remarkably different, in spite of their structural similarity.

Introduction

Investigation of the kinetics of molecular movements in solutions can provide interesting information on intermolecular interactions, solvation mode, association, and related phenomena. One of the most efficient experimental methods of such investigations is based on interpretation of the nuclear spin relaxation data. In the literature one can find numerous examples of successful application of this method.^{1–6} Most frequently, the dipolar contribution to the overall longitudinal relaxation rates and NOE enhancement factors are used in such studies as a source of information on the molecular dynamics. The only additional molecular property necessary to interpret such data is the molecular geometry. During a detailed interpretation of the dipolar relaxation rates, however, the vibrational averaging of the involved dipolar couplings has to be taken into account, which causes some complications to arise.^{7–15} Moreover, the number of independent data is sometimes insufficient for unambiguous determination of the rotational diffusion tensor.^{16,17} The relaxation data set can be, and sometimes has to be, enlarged by including the relaxation rates due to other than dipolar mechanisms and other than R_1 or η relaxation parameters.^{4,17–24} In the case of the molecule including nuclei possessing spins higher than 1/2 their relaxation rates due to the quadrupole mechanism are a convenient information source. In this case the electric field gradient (EFG) tensors at particular nuclear sites are necessary for the interpretation of the relaxation data. Presently, both the molecular geometries and EFG tensors can

be calculated theoretically with a sufficient accuracy for medium size molecules, using widely accessible quantum chemistry programs. Actually, the calculation results can sometimes be more adequate than the available experimental ones, since the mentioned molecular properties should concern molecules in the solution that is the same situation as that occurring during the relaxation measurements. Determination of the molecular geometry and especially EFG tensors, however, is usually impossible for molecules in solutions, and the available experimental results normally concern the solid or gaseous state.

In most investigations of the molecular reorientation in solution by the nuclear spin relaxation measurements the authors assumed the isotropic or axially symmetrical reorientation of the investigated molecule, and only very few of them adopted the symmetry of the rotational diffusion tensor being in full agreement with the symmetry of the solute molecule.² Such practice was probably caused by the fact that the mathematical description interconnecting a fully anisotropic rotational diffusion tensor and particular interaction tensors with measurable relaxation parameters is rather complicated.^{16,25–27} Furthermore, even for rigid molecules this formalism involves up to 6 parameters defining the diffusion tensor which eventually have to be determined. At the same time, the number of independent and sufficiently accurate relaxation data is usually limited. In consequence, the involved set of equations can have multiple solutions being not very different from each other and poorly conditioned in the least-squares sense.²⁸ The selection of the correct solution, the control of its uniqueness, and the evaluation of its credibility can be nontrivial tasks. It seems, however, that all the above obstacles have already been broken through by

* To whom correspondence should be addressed. E-mail: agryff@ch.pw.edu.pl.

various authors and efficient ways of overcoming most of these problems have been proposed. The mathematical description of the problem was reformulated by Canet,²⁷ who implemented Werbelow's idea of splitting the asymmetrical interaction tensors into pairs of axially symmetrical tensors with symmetry axes directed along z and x principal axes of the initial tensors.²⁹ The obtained formulas have the form suitable for programming. Finally, it seems that the problem of credibility and uniqueness of the solution found can be tested by using a Monte Carlo method.^{28,30–32}

Keeping in mind the perspective of applying this method to study the behavior of nucleic bases and nucleosides in solutions, we decided to check the practicability of all the procedure choosing as the test examples 9-methylpurine (**1**) and 7-methylpurine (**2**). To simplify the quantitative interpretation of the relaxation data, we investigated the isotopomers of these compounds deuterated in methyl groups. The selected compounds seem to be especially suitable for testing purposes. Their molecules possess the symmetry plane and are rigid if one neglects the methyl group rotation. Thus, the reorientation of these molecules can be adequately and completely described within the rotational diffusion theory of asymmetrical top.² Additionally, the direction of one of the principal diffusion axes is known a priori and only three diffusion coefficients (principal values of the diffusion tensor) and the angle defining the directions of in-plane diffusion axes have to be determined.² The selected molecules are at the same time of the size enabling the reliable theoretical calculation of their geometries and EFG tensors at nitrogens, which are all the necessary molecular parameters needed for the interpretation of the relaxation data. Below we report the results of our investigation of the selected purine derivatives **1** and **2** involving determination of the ¹⁴N and ¹³C relaxation rates followed by their interpretation in the frame of the anisotropic rotational diffusion theory. The reliability of the final results has been tested by a Monte Carlo method. This study confirms once again that careful interpretation of relaxation data can provide a lot of interesting and unique information concerning the solution behavior and solvation of molecules.

Experimental Section

9-(Trideuteromethyl)purine (**1**) and 7-(trideuteromethyl)purine (**2**) were synthesized by methylation of purine (98+%, Aldrich) with CD₃I (99.5 atom % D, Aldrich) and chromatographic separation of isomers using the literature procedure.³³

NMR measurements were performed for samples containing 1.3, 0.56, and 0.13 M of **1** in CD₃OD, for samples of 0.61 and 0.13 M CD₃OD solutions of **2** and the sample containing the mixture of 0.52 M of **1** and 0.31 M of **2**. All samples were prepared directly in 5 mm o.d. NMR tubes, degassed, and sealed. All the spectra were recorded at 30 °C; the measurement temperature was stabilized using spectrometer VT devices and controlled by the ethylene glycol sample. ¹⁴N NMR spectra were recorded at $B_0 = 11.7$ T magnetic field by Bruker Avance DRX 500 spectrometer; nitrogen chemical shifts were referenced via spectrometer frequency to the independently measured signal of CH₃NO₂. ¹H NMR and ¹³C NMR spectra were recorded using Varian Mercury 400 spectrometer ($B_0 = 9.4$ T). Longitudinal ¹H and ¹³C relaxation times were measured by inversion–recovery, ¹³C{¹H} NOE enhancement factors by dynamic NOE,^{34,35} and ¹H transverse relaxation times by CPMG techniques. The three-parameter fit was used to retrieve the relaxation parameters from the signal intensity vs recovery delay dependence or the two parameter fit in the case of CPMG data.

NOE enhancement factors were also determined using the classical method on the basis of comparison of the signal intensities in the spectra of the sample in the equilibrium states with and without proton decoupling during the sufficiently long ($\sim 10/R_1$) relaxation delay. All these relaxation measurements were performed at least three times, and the arithmetical averages of their results are given in tables.

All quantum chemical calculations were performed using the Gaussian 03W program.³⁶ The computer program enabling retrieving the rotational diffusion parameters from the relaxation data and the programs for inversion–recovery and CPMG data fitting and for line shape analysis of ¹⁴N NMR spectra were written in GNU Fortran and were based on the Newton–Raphson algorithm of iterative nonlinear least-squares sum minimization. The program for relaxation data analysis was based on the formulation of relaxation equations given by Canet.²⁷ The input data were composed of the following: (I) molecular geometry; (II) block defining dipolar interactions (numbers of interacting atoms and their mass numbers); (III) block defining CSA interactions (number of atom, its mass number, and its shielding tensor); (IV) block defining quadrupole interactions (number of atom, its mass number, and appropriate EFG tensor); (V) starting values of diffusion coefficients and f factor (see Results and Discussion); (VI) block containing experimental relaxation data with information on relaxation mechanisms and the magnetic field used in the measurements. The data introduced in points I, III, and IV were given in the Gaussian format. The values of the nuclear spins, quadrupole moments, and magnetogyric ratios were contained in the “block data” of the program.

Results and Discussion

Relaxation Mechanisms. Taking into account the structure of the investigated compounds, one may consider five magnetic isotopes which could be used as probes of molecular motion. Certainly, the measurements for protons (¹H) are the easiest to perform, because of the highest NMR sensitivity of this isotope. Unfortunately, in the case of the longitudinal relaxation of the proton signals, the intermolecular relaxation mechanisms, which are difficult to interpret in detail, play usually a substantial role. Nevertheless, two types of measurements involving protons have been done in this work. Namely, the longitudinal relaxation of ¹³C satellites could be interpreted, as it was dominated by the dipolar ¹³C–¹H relaxation mechanisms. Moreover, the transverse ¹H relaxation caused mainly by the scalar relaxation of the second kind was used as a source of information on the relaxation rates of nitrogens. Two other isotopes, ²H and ¹⁵N, can be exploited in relaxation studies in practice only after sufficient isotope enrichment, because of their low natural abundances and nuclear magnetic moments. In consequence, most of this work is dealing with the interpretation of the relaxation measurements of ¹³C and ¹⁴N nuclei.

Relaxation rates obtained from experiments for particular magnetic nuclei are always sums of contributions coming from several elementary relaxation mechanisms.³⁷ However, taking into account the structures of the investigated molecules, their size, the magnetic fields used, and other measurement conditions, one may predict the relative importance of various mechanisms for particular nuclei. These predictions, based on general considerations concerning nuclear spin relaxation phenomena, could be verified a posteriori by calculating the contributions of particular mechanisms to the overall relaxation, using the rotational diffusion parameters determined earlier (Table 1).

TABLE 1: Contributions of Particular Relaxation Mechanisms to the Overall Relaxation Rates of the Atomic Nuclei in 9-Methylpurine Calculated Using the Rotational Diffusion Parameters for the Sample 1a Containing 1.3 M Solution of the Base and Assuming $B_0 = 9.4$ T and Theoretically Calculated Molecular Parameters

nucleus	R_{1DD}			R_{1Q}	R_{1CSA}^a	ΣR_1 calcd	R_1 exptl
	adjacent 1H	remote 1H	^{14}N				
^{14}N -1		0.0011		4815	0.0107	4815	4890
^{14}N -3		0.0007		3416	0.0095	3416	3450
^{14}N -7		0.0007		2669	0.0077	2669	2630
^{14}N -9		0.0005		1392	0.0014	1392	1390
^{13}C -2	0.2817	0.0005	0.0031		0.0172	0.3025	0.322
^{13}C -4		0.0015	0.0029		0.0184	0.0228	≈ 0.025
^{13}C -5		0.0071	0.0012		0.0141	0.0224	≈ 0.025
^{13}C -6	0.2885	0.0005	0.0013		0.0198	0.3101	0.314
^{13}C -8	0.3306	0.0002	0.0029		0.0113	0.3450	0.357

^a For corresponding calculated magnetic shielding tensors data, see Supporting Information.

Thus, it was evident that the relaxation of all ^{14}N nuclei was completely dominated by the quadrupole mechanism and the effects of other mechanisms could be safely neglected. Moreover, in the case of ^{14}N nuclei the tumbling of the solute molecules was probably the only type of motion causing relaxation. Indeed, the results of the calculations described below have shown that the formation–decomposition process of the hydrogen-bonded complexes introduces an additional fluctuation of quadrupole energy. The amplitude of this fluctuation, however, being proportional to ΔEFG is small and amounts only to at most 10% of the total quadrupole energy. Remembering that the relaxation rate is proportional to the square of the involved fluctuation amplitude, one may conclude that the contribution of the discussed process to the overall relaxation rate is insignificant, independent of the lifetime of the hydrogen-bonded complexes.

The relaxation of ^{13}C nuclei represented a somewhat more complicated case. For the protonated carbons (C-2, C-6, and C-8) the dipolar relaxation was the most effective, though not the only operating mechanism. For the quaternary carbons (C-4 and C-5), the mechanism due to the shielding anisotropy was expected to play an important role, especially at higher magnetic fields. The contribution of any intermolecular mechanisms to the longitudinal relaxation of ^{13}C nuclei of both types was expected to be a minor part of the overall relaxation rate, as we were dealing with diamagnetic systems and solutions in the deuterated solvent. Nevertheless, the direct quantitative interpretation of the total ^{13}C relaxation rates obtained from measurement was impossible in practice, because of multiple minor contributions coming from various relaxation mechanisms. The standard strategy in such a situation is the initial separation of the contribution due to a given mechanism from the total relaxation rate, followed by its interpretation in terms of diffusion parameters.³⁷ In this work we decided to exploit only the dipolar relaxation of the protonated carbons.

Calculation of Molecular Parameters. For the quantitative interpretation of the relaxation data in terms of correlation times or rotational diffusion parameters, the molecular geometries of the investigated compounds and the quadrupole coupling tensors of their nitrogen nuclei were needed. Since the relaxation data were measured for molecules in solutions, it was important to ensure that the values of other molecular parameters referred to the same conditions. It seemed almost certain that in the methanol solution we were dealing with the solute molecules forming hydrogen-bonded complexes in which the lone electron pairs of N-1, N-3, and N-7 of 9-methylpurine or N-1, N-3, and N-9 nitrogens of 7-methylpurine were complexed by solvent molecules.³⁸ The molecular geometries of trimethanولات of 9-methylpurine and 7-methylpurine were found optimizing the

total energy using DFT approach as implemented in Gaussian 03 program³⁶ with the B3LYP functional and 6-311++G(2d,p) basis set. The impact of bulk solvent on the electronic structure of such agglomerates was taken into account using the polarizable continuum model³⁹ during the calculations. It is to be realized that solvates by their nature have very labile structures, and in solution various solvate forms and conformers are simultaneously present and rapidly interconvert one into another. We were aware that the found geometries of the solute trimethanولات were referred probably to local rather than global energy minima. Nevertheless, we believe that EFG tensors (calculated in the next step) for the found species represent better approximations of these properties of the solute molecules in the solution than values calculated for unsolvated molecules. More adequate description of the real situation could be probably gained by using the molecular dynamics methods.

It was shown that quadrupole coupling tensors for nitrogen-14 nuclei could be calculated theoretically for isolated molecules with the accuracy of the order of 1.3%, which was probably higher than that obtainable in standard experiments.⁴⁰ To achieve such results, Bailey⁴⁰ employed the high level of theory [DFT B3PW91/6-311+G(df,pd)] and performed a careful calibration of his method. Namely, he selected a series of reference compounds whose molecular geometries and quadrupole coupling tensors had been known from measurements and calculated for them the EFG tensors. Then he performed the linear regression between the principal components of these tensors and the components of the experimental e^2Qq/h tensors. The correlation was perfect, with the intercept close to zero. The slope of the regression line (4.5617(43) MHz/au) essentially ought to have been equal to eQ/h , Q being the quadrupole moment of ^{14}N nucleus. Actually, the above number included the correction compensating for the influence of molecular vibrations on the experimental e^2Qq/h values, as well as for any systematic imperfections of the theoretical method. Thus, the determined value of $(eQ/h)_{\text{eff}} = 4.5617$ MHz/au was considered to be the scaling factor calibrating the method.

We applied the above method to calculate quadrupole coupling tensors for nitrogens in the investigated compounds. The unavoidable divergence from the original method was the fact that we had to use the calculated rather than experimental molecular geometries. To examine the possible consequences of this modification, we performed the appropriate calculations for isolated molecules of pyridine and imidazole (Table 2) (included by Bailey into the reference series) using the optimized molecular geometries. Some minor differences between our results and that obtained for experimental geometries were evident, but the found mean value of the calibration factor, $(eQ/h)_{\text{eff}} = 4.5345$ MHz/au, was close to that determined in ref 40.

TABLE 2: Electric Field Tensors (in au) at Nitrogen Nuclei in Pyridine, Imidazole, and Investigated Methylpurines in the Gas Phase and in Methanol Solution Calculated by the DFT B3PW91/6-311+G(df,pd) Method

compd	EFG (gas phase)			EFG (PCM, methanol)			EFG (PCM, methanol, with methanol complexes)		
	3XX-RR	3YY-RR	3ZZ-RR	3XX-RR	3YY-RR	3ZZ-RR	3XX-RR	3YY-RR	3ZZ-RR
pyridine	1.085 117	-0.320 340	-0.764 777	1.021 284	-0.319 465	-0.701 818	0.904 164	-0.308 898	-0.595 265
imidazole N-1	-0.290 469	-0.268 588	0.559 058	-0.236 940	-0.207 748	0.444 688	-0.240 751	-0.172 613	0.4133 64
imidazole N-3	0.884 692	-0.388 609	-0.496 083	0.791 691	-0.383 744	-0.407 947	0.713 791	-0.307 344	-0.406 446
9-methylpurine N-1	1.018 553	-0.372 921	-0.645 631	0.964 677	-0.375 193	-0.589 483	0.862 966	-0.360 531	-0.502 435
9-methylpurine N-3	-0.152 933	0.703 009	-0.550 077	-0.164 188	0.690 029	-0.525 841	-0.012 955	0.470 938	-0.457 983
9-methylpurine N-7	-0.425 440	0.826 585	-0.401 146	-0.439 981	0.767 208	-0.327 227	-0.361 394	0.637 678	-0.276 284
9-methylpurine N-9	-0.332 148	-0.326 280	0.658 428	-0.321 079	-0.289621	0.610 700	-0.313 792	-0.271 744	0.585 536
7-methylpurine N-1	0.185 181	0.465 666	-0.650 847	0.160 156	0.431 863	-0.592 019	0.2087 83	0.523 685	-0.732468
7-methylpurine N-3	-0.115 205	0.785 868	-0.670 663	-0.136 697	0.722 593	-0.585 897	-0.197 308	0.521 084	-0.323 775
7-methylpurine N-7	-0.380 924	-0.328 704	0.709 628	-0.350 837	-0.280 220	0.631 057	-0.340 479	-0.270 449	0.610 929
7-methylpurine N-9	-0.407 883	0.822 179	-0.414 296	-0.430 235	0.742 440	-0.312 205	-0.245 010	0.498 004	-0.252 993

TABLE 3: Comparison of the Relaxation Rates for Particular Nuclei of 9-(Trideuteromethyl)purine Measured for Its Methanol-*d*₄ Solutions with the Values Calculated Using the Found Optimal Values of Rotational Diffusion Parameters (Table 5)^a

nucleus	mechanism	sample 1a				sample 1b		sample 1c		sample 1d	
		expt	calcd	calcd _{iso}	$\tau_{\text{eff}}/\text{ps}$	expt	calcd	expt	calcd	expt	calcd
¹⁴ N-1	R _{2Q}	4890	4820	3930	19	4280	4320	3460	3460		4740
¹⁴ N-3	R _{2Q}	3450	3420	3460	15	3180	3130	2560	2560		3170
¹⁴ N-7	R _{2Q}	2630	2670	2580	16	2420	2460	1950	1950		2520
¹⁴ N-9	R _{2Q}	1390	1400	1740	12	1210	1210	1030	1030		1380
¹³ C-2	R _{1DD}	0.288	0.285	0.283	16	0.259	0.260		0.201	0.276	0.276
¹³ C-6	R _{1DD}	0.287	0.290	0.282	16	0.265	0.264		0.217	0.268	0.268
¹³ C-8	R _{1DD}	0.326	0.333	0.286	18	0.306	0.301		0.233	0.331	0.331
¹ H-2 ^b	R _{2SC2}	1.62	1.60				1.77		2.18	1.69	1.69
¹ H-8 ^b	R _{2SC2}	1.45	1.48				1.65		2.02	1.54	1.54

^a The column "calcd_{iso}" contains the optimum values for the isotropic reorientation model ($\tau_{\text{iso}} = 16$ ps, $D_{\text{iso}} = 10.76 \times 10^9$ s⁻¹), and the column " τ_{eff} " contains the effective reorientation correlation times calculated from particular relaxation data assuming isotropic reorientation. ^b Calculated theoretically ²*J*(¹⁴N-¹H) coupling constants and (in parentheses) values recalculated from the appropriate ¹⁵N-¹H couplings measured using ¹H-¹⁵N HMQC correlation: ²*J*(N-1-H-2), 10.6 Hz (11.1 Hz); ²*J*(N-1-H-6), 7.5 Hz (7.8 Hz); ²*J*(N-3-H-2), 11.0 Hz (11.0 Hz); ²*J*(N-7-H-8), 8.5 Hz (8.9 Hz); ²*J*(N-9-H-8), 5.8 Hz (6.1 Hz).

Taking into account that the statistics standing behind our value were much poorer than those behind the original one, we decided to use the latter in further calculations. Additionally, to estimate the importance of solvent on QCC, we performed calculations for the above two test molecules and also for their hydrogen-bonded complexes with methanol, simulating the influence of the bulk solvent by the polarizable continuum model (PCM). The analogous calculations were performed for the investigated methylpurines. The data collected in Table 2 clearly show that the solvent does affect the electron density distribution in the solute. Neglecting this fact and using EFG tensors calculated for isolated molecules during the interpretation of the relaxation data would thus introduce significant errors. Recently, the substantial influence of the intermolecular hydrogen bonding on nitrogen quadrupole coupling tensors in 9-methyladenine was evidenced by Mirzaei and Hadipour.⁴¹

Finally, using the same level of theory and the GIAO method, the magnetic shielding tensors and scalar coupling constants of atomic nuclei in the investigated compounds were calculated. In the last part of this work these tensors were used for evaluating the contributions of CSA mechanism to the overall relaxation of particular nuclei (Table 1). The two-bond ¹H-¹⁴N scalar coupling constants were needed for interpretation of the proton relaxation data.

Relaxation Rates Determination. Our relaxation measurements were performed for three samples, **1a-c**, containing 1.3, 0.56, and 0.13 M solutions of **1** and for two samples, **2b,c**, containing 0.61 and 0.13 M of **2**. Moreover, we investigated the sample **1d + 2d**, containing the mixture of **1** and **2** in proportion of ca. 1.68:1 and overall solute concentration of ca. 0.83 M. During the investigation of this sample some problems

arose due to superposition of the ¹⁴N spectra, but the crucial advantage was that the measurement conditions for two investigated solutes were identical.

The relaxation rates of ¹⁴N nuclei in the investigated methylpurines (in all samples but **1d + 2d**) were determined from the line widths of the signals in their ¹⁴N NMR spectra. These signals were assigned to particular nitrogens in methylpurine structures on the basis of 2D ¹H-¹⁵N HMQC spectra. The transverse ¹⁴N relaxation rates, *R*₂, were calculated from the half-height line widths, *w*, using the formula³⁷

$$R_2 = \pi w \quad (1)$$

In the applied measurement conditions all nitrogen signals were broad (hundreds of hertz) for the investigated samples and the spectrometer field inhomogeneity being of the order of 1 Hz was meaningless for the measurement precision. In the spectra, which were measured at 11.7 T magnetic field, some signals strongly overlapped one another (Figure 1) and in every case the determination of the line widths demanded applying the numerical analysis of the line shapes. In these analysis the Lorentzian shape of the spectral lines was assumed, and in the most difficult cases the additional constraints concerning some of the chemical shift differences had to be imposed during the fitting procedure. The necessary information concerning nitrogen chemical shifts had been taken from 2D ¹H-¹⁵N HMQC spectra. The obtained results were collected in Tables 3 and 4. Comparison of the data for different samples and further analysis of all the relaxation data showed that only in the case of the broadest signal of N-1 in the sample **2b** the appropriate line width had been estimated with lesser precision, probably of the

TABLE 4: Comparison of the Relaxation Rates for Particular Nuclei of 7-(Trideuteromethyl)purine Measured for its Methanol-*d*₄ Solutions with the Values Calculated Using the Found Optimal Values of Rotational Diffusion Parameters (Table 5)^a

nucleus	mechanism	sample 2b				sample 2c		sample 2d	
		expt	calcd	calcd _{iso}	$\tau_{\text{eff}}/\text{ps}$	expt	calcd	expt	calcd
¹⁴ N-1	R _{2Q}	3630	4260	4280	14	4850	4900		4470
¹⁴ N-3	R _{2Q}	4220	4340	4070	18	4280	4230		4680
¹⁴ N-7	R _{2Q}	1390	1390	1990	12	1540	1530		1540
¹⁴ N-9	R _{2Q}	3080	3140	2710	19	3350	3210		3330
¹³ C-2	R _{1DD}	0.324	0.325	0.311	17	0.295	0.295	0.342	0.344
¹³ C-6	R _{1DD}	0.348	0.344	0.309	19	0.337	0.341	0.372	0.369
¹³ C-8	R _{1DD}	0.325	0.322	0.313	18		0.325	0.340	0.337
¹ H-2 ^b	R _{2SC2}	2.08	1.54				1.45	1.69	1.44
¹ H-8 ^b	R _{2SC2}	1.83	1.34				1.26	1.20	1.24

^a The column “calcd_{iso}” contains the optimum values for the isotropic reorientation model ($\tau_{\text{iso}} = 17$ Ps, $D_{\text{iso}} = 9.76 \times 10^9 \text{ s}^{-1}$), and the column “ τ_{eff} ” contains the effective reorientation correlation times calculated from particular relaxation data assuming isotropic reorientation. ^b Calculated theoretically ² $J(^{14}\text{N}-^1\text{H})$ coupling constants: ² $J(\text{N}-1-\text{H}-2)$, 10.7 Hz; ² $J(\text{N}-1-\text{H}-6)$, 7.1 Hz; ² $J(\text{N}-3-\text{H}-2)$, 10.5 Hz; ² $J(\text{N}-7-\text{H}-8)$, 5.4 Hz; ² $J(\text{N}-9-\text{H}-8)$, 8.5 Hz.

order of 15%. In all other cases the procedure seemed to be accurate within 5%.

The above method could not be applied to the sample **1d** + **2d** containing a mixture of the investigated compounds. In this case the information on nitrogen relaxation rates was gained indirectly via the transverse relaxation rates of ¹H nuclei. The latter were measured using the classical CPMG experiment (taking into account the influence of the echo time, t_{cp}).⁴² The information desired could be drawn because the contribution of the scalar relaxation of the second kind to the transverse relaxation of protons scalar-coupled to ¹⁴N was dominant. In practice this relaxation rate is inversely proportional to the longitudinal relaxation rate of the involved nitrogen:³⁷

$$R_{2A,SC2} = \frac{4}{3} \pi^2 J^2 I_X (I_X + 1) \left(\frac{1}{R_{1X}} + \frac{R_{2X}}{R_{2X}^2 + \Delta\omega^2} \right) \approx \frac{4}{3} \frac{\pi^2 J^2 I_X (I_X + 1)}{R_{1X}} \quad (2)$$

where A = ¹H and X = ¹⁴N. Since the SC2 mechanism practically does not affect the longitudinal relaxation of protons coupled to ¹⁴N, the conventional procedure used for the separation of SC2 contribution to R_2 relies upon performing the measurements of R_2 and R_1 for a given proton and then exploiting the equation

$$R_{2SC2} = R_2 - R_1 \quad (3)$$

It has to be remembered, however, that this procedure is very susceptible to various experimental errors and also to the presence of traces of paramagnetic species in the investigated solution. To check the reliability of all the procedure, we performed the measurements of proton relaxation rates for the sample **1a** containing 1.3 M solution of **1**, which was independently investigated by ¹³C and ¹⁴N relaxations. The results of the analysis of the latter data were used to calculate the SC2 relaxation rates of protons, and the obtained values were collected in Table 3. The comparison of these values with the experimental ones showed that the relaxation rates of H-2 and H-8 were reproduced satisfactorily, whereas, for H-6 of the slowest relaxation (due to interaction with only one nitrogen), the noticeable divergence did appear. Consequently, we decided to exclude the data for H-6 during the analysis of the **1d** and **2d** data sets.

The dipolar longitudinal relaxation rates, R_{1DD} , of protonated carbons were determined in three independent ways. The first

method, applied to all samples except **1c**, was the combination of the results of the conventional inversion–recovery experiment with the permanent proton decoupling and the NOE factors, η , measured by comparing the signal intensities in the fully relaxed spectra with and without proton decoupling during the relaxation delay. To obtain the dipolar contribution, R_{1DD} , to the total relaxation rate, R_1 , the well-known dependence was used:³⁷

$$R_{1DD} = \frac{\eta}{\eta_{\text{max}}} R_1 \quad (4)$$

Anticipating the results of our relaxation data analysis, we assumed that in the applied experimental conditions the solute molecules underwent fast reorientation ensuring the extreme narrowing limit. In such a case the maximum value of the NOE factor amounts to

$$\eta_{\text{max}} = \frac{1}{2} \frac{\gamma_{\text{H}}}{\gamma_{\text{C}}} = 1.988 \quad (5)$$

Usually, in the above approach, the determination of the precise values of NOE coefficients becomes the bottleneck for the quantitative interpretation of the relaxation data. Thus, we additionally performed the dynamic NOE experiment ($d > 5/R_1$ (decoupler off), variable τ (decoupler on), pw 90°, acquisition (decoupler on)).^{34,35} This experiment is more time-consuming than the first method but allows avoiding the consequences of

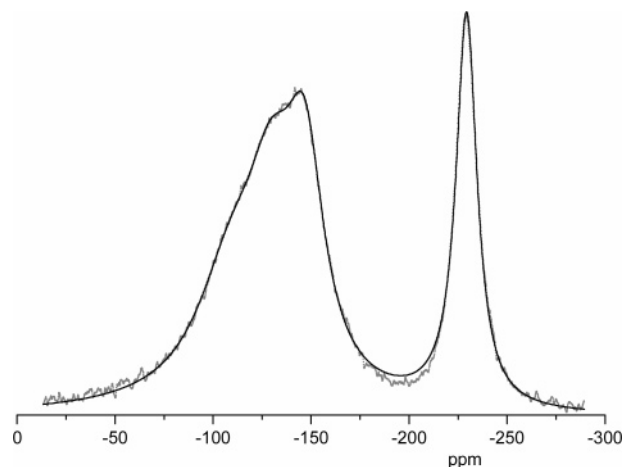


Figure 1. Line shape analysis of ¹⁴N NMR spectrum of 9-methylpurine (sample **1a**): dots for experimental spectrum; smooth line for theoretical spectrum found.

pulse imperfections. The results obtained with both methods were very similar. However, when during the dynamic NOE data analysis the longitudinal relaxation rates were assumed to be exactly equal to those obtained from the inversion–recovery experiment, the calculated NOE coefficients were usually slightly higher than those from the standard method based on signal intensities in only two spectra.

Finally, for the 1.3 M solution of **1** and 0.61 M solution of **2** (samples **1a** and **2b**), if one takes advantage of the simplicity of the proton spectra, the relaxation rates due to the same dipolar ^{13}C – ^1H interactions were determined from the ^1H NMR inversion–recovery experiment with carbon-13 decoupling during the evolution delay. For a given proton, $R_{1\text{DD}}$ was determined as a difference between the recovery rate of ^{13}C satellites and the recovery rate of the central signal. These two rates had to be measured in separate experiments, because they were very different. To be specific, contrary to the previous methods, the relaxation rate measured this way was not influenced by dipolar interactions with remote protons. In the case of carbon these interactions were, however, so weak as compared to the interaction with the directly bonded proton that the appropriate contributions to the overall relaxation vanished in the experimental errors and the obtained results were practically identical with those obtained by two other methods. The obtained dipolar relaxation rates of C-2, C-6, and C-8 carbons of the investigated methylpurines were collected in Tables 3 and 4.

Summarizing, we collected 3 experimental data sets (**1a,b** and **2b**), each composed of 7 independent relaxation data: 4 quadrupole relaxation times for nitrogens and 3 longitudinal dipolar relaxation times for protonated carbons. For the most dilute sample of 9-methylpurine (**1c**), only the transverse ^{14}N relaxation rates were determined. In the case of sample **2c** $R_{1\text{DD}}$ for C-8 was not determined because of partial deuteration at this position before completion of all the measurements. Moreover, for the sample containing the mixture of both investigated compounds, two data sets, **1d** and **2d**, each composed of three dipolar relaxation rates for C-2, C-6, and C-8 and two transverse relaxation rates for H-2 and H-8, due to scalar relaxation of the second kind, dependent on the appropriate linear combinations of $R_{1\text{Q}}$ of nitrogens were collected. All the above data are collected in Tables 3 and 4.

Relaxation Data Analysis. In the case of isotropic molecular reorientation, which is the simplest for a formal treatment, the equations describing relaxation rates due to single elementary nuclear interaction x assume the form³⁷

$$R_{1,x} = k_x^2 j_x(\omega_0, \tau_c) \quad (6)$$

where j_x is a specific combination of the spectral densities of correlation functions describing the energy fluctuation of a given interaction, ω_0 is the appropriate Larmor frequency at the spectrometer magnetic field, τ_c is the reorientation correlation time, and k_x^2 represents the mean square amplitude of the energy fluctuation involved. In the case of quadrupole and dipolar relaxation mechanisms considered in this work the latter parameter has a form

$$k_{\text{Q}}^2 = \frac{3}{10} \pi^2 \frac{2I+3}{I^2(2I-1)} \left(\frac{e^2 Q q_{zz}}{h} \right)^2 \left(1 + \frac{\eta^2}{3} \right) \quad (7)$$

$$k_{\text{A,DD}}^2 = \frac{4}{3} I_{\text{B}} (I_{\text{B}} + I) \left(\frac{\mu_0 \gamma_1 \gamma_2 \hbar}{4\pi r_{\text{AB}}^3} \right)^2 \quad (8)$$

where $e^2 Q q_{zz}/h$, η , and r_{AB} are the quadrupole coupling constant, asymmetry parameter of EFG tensor, and effective distance between A and B nuclear dipoles, respectively. Other symbols in eqs 7 and 8 have their usual meanings. In the fast reorientation limit, valid for methylpurines in our samples (see below), eq 6 simplifies remarkably, because³⁷

$$j_x(\omega_0, \tau_c) = \tau_c \quad (9)$$

and for both mechanisms the longitudinal and transverse relaxation rates become equal:

$$R_{1,x} = R_{2,x} \quad (10)$$

For anisotropic reorientation of the molecules, the latter property is still valid for DD and Q mechanisms, as is the independence of relaxation rates of B_0 , as long as the extreme narrowing condition is obeyed. In this case the detailed description of the relaxation phenomenon becomes, however, very complex. Probably the most compact (but still complicated) description of the relaxation due to a general anisotropic interaction tensor undergoing anisotropic reorientation was proposed by Canet and used in this work.

From the above outline of the relaxation theory it is clear that for any interpretation of the relaxation data concerning the quadrupole mechanism the EFG tensors at quadrupole nuclei are necessary. The way of calculating them was presented in one of the former paragraphs. We remind that the applied calibration procedure of the theoretical data ensures the automatic compensation for the ground-state vibrational motions. On the other hand, the dipolar coupling constants, needed for interpretation of the dipolar relaxation rates calculated from the optimum molecular geometries, still require correcting to include consequences of such motions. The vibrational motions are too fast to cause relaxation, but they do reduce the effective dipolar constants. Such corrections play a role only for short distances between interacting nuclei, e.g., when ^{13}C nucleus interacts with the proton bonded to it, but actually, it is the most frequently encountered situation. It seems that there is no commonly accepted procedure of including vibrational effects into the interpretation of the relaxation data.^{7–15} In some works they were simply neglected, in spite of the known, pronounced, and systematic errors introduced by such an approximation. Some authors proposed to use the effective distances calculated with the formula

$$r_{\text{eff}} = r_e + \langle \Delta_z \rangle - \frac{2}{r_e} \langle \Delta_z^2 \rangle + \frac{1}{2r_e} (\langle \Delta_x^2 \rangle + \langle \Delta_y^2 \rangle) \quad (11)$$

where $r_e = |\mathbf{r}_e|$ is the equilibrium distance, Δ is a vector defined by $\Delta = \mathbf{r}(t) - \mathbf{r}_e$, and the brackets denote averaging over the vibrational motion. The effects of unharmonic and harmonic stretching vibrations are described by $\langle \Delta_z \rangle$ and $\langle \Delta_z^2 \rangle$, respectively, whereas the effects of bending vibrations are described by $\langle \Delta_x^2 \rangle + \langle \Delta_y^2 \rangle$. For example, according to Dölle et al.,¹¹ this procedure increases the equilibrium distance $r_e(\text{C–H}) = 108$ pm in benzene to $r_{\text{eff}}(\text{C–H}) = 110.6$ pm ($f = r_{\text{eff}}/r_e = 1.024$). It seems, however, that the procedure based on eq 11 still somewhat underestimates the overall effect of ultrafast motions, as the relaxation measurements as well as the uncorrected residual dipolar coupling constants determined for partially oriented molecules have permanently yielded larger C–H distances (112–115 pm).^{8,12,14,15} In this work, during the interpretation of the relaxation data, to include the vibrational

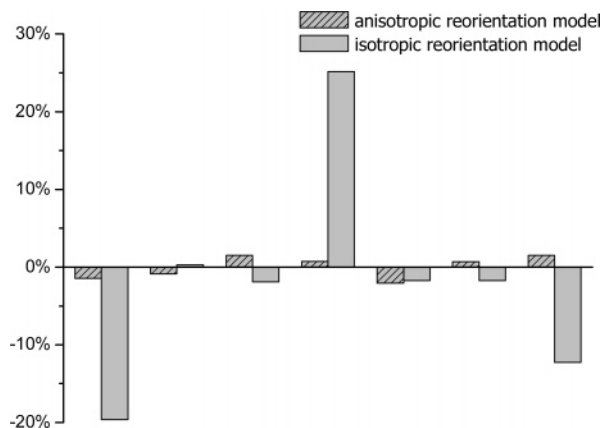


Figure 2. Comparison of the effectiveness of isotropic and anisotropic reorientation models in reproducing the experimental relaxation data obtained for 9-methylpurine (sample **1a**). (Bars denote relative errors of particular data points.)

effects into the data analysis, all the C–H bonds were artificially enlarged by the factor f relative to optimum geometry (see below).

At the initial stage of the elaboration of the experimental data a crude analysis was performed, based on the assumption that the rotational diffusion of solute molecules was isotropic. At least two different approaches were essentially possible within this assumption. First, the effective correlation time can be calculated from every single relaxation rate using eqs 6–8. Those correlation times, more or less directly, characterize the kinetics of the energy fluctuation of the appropriate elementary interaction leading to the relaxation of a given nucleus. The results of such a procedure applied to the two most concentrated samples **1a** and **2b** are collected in the appropriate columns of Tables 3 and 4. Inspection of these results has shown that the tumbling rates of both solute molecules are really fast so that the extreme narrowing condition is fulfilled. Moreover, the substantial spread of the calculated effective correlation times points out that the isotropic reorientation model poorly describes the real situation in the investigated cases. Second, all the data measured for a given sample were analyzed simultaneously to find the correlation time being the best in the least-squares sense. This way of analysis allowed us to compare the effectiveness of reproducing experimental data by the isotropic reorientation model and by the anisotropic model discussed below. The prevalence of the latter was evident (Figure 2).

As it was mentioned in the Introduction, taking into account molecular symmetry, the reorientation of the investigated methylpurine molecules in solution should be described by the rotational diffusion theory of an asymmetrical planar top. Within this formalism a relaxation parameter measured for a magnetic nucleus of the investigated molecule can be expressed as a function of the appropriate physical constants, molecular parameters, three rotational diffusion coefficients, and the angle α defining the orientation of the in-plane diffusion axes. During the relaxation data analysis the last four parameters were unknowns. Additionally, in some initial runs the value of the scaling factor, f , which modifies the C–H bond lengths, introduced to compensate the effect of ground-state vibrations was determined. This factor was assumed to be the same for all C–H bonds in a given molecule in a given sample. Five of our relaxation data sets allowed determining the value of this factor. The values of f obtained for various data sets were 1.024–1.036. On the other hand, it seemed hardly probable that vibrational effects for two investigated molecules or different samples were different. Thus, to get the diffusion parameters

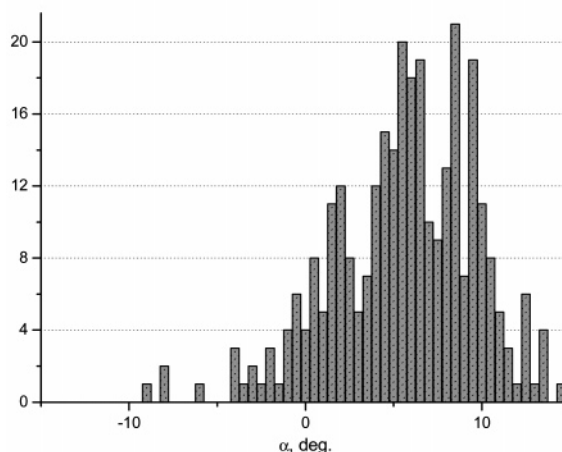
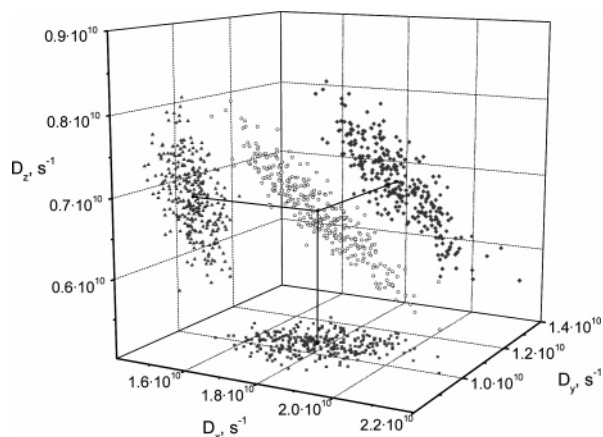


Figure 3. Illustration of the Monte Carlo simulation of the sensitivity of the diffusion parameters to the errors of the experimental relaxation data. The results concern the sample **1a**.

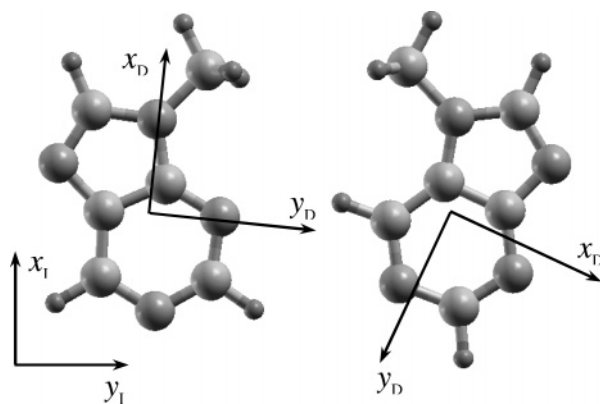


Figure 4. Orientation of the in-plane diffusion and inertia axes for the investigated compounds (samples **1a** and **2b**, respectively).

suitable for comparison, in the final step the relaxation data were analyzed once again assuming the same value $f = 1.030$ for all the investigated samples. The obtained diffusion parameters are shown in Table 5. The adopted value of f yielded the effective C–H bond lengths for the investigated compounds in the range 111.9–112.2 pm.

The numerical problem to be solved during our relaxation data analysis amounted to solving the system of 7 (samples **1a,b** and **2b**), 6 (**2c**), 5 (**1d** and **2d**), or 4 (**1c**) equations and 4 or 5 unknowns. In the case of samples **1d**, **2d**, and **1c** the value of the factor f was not fitted. In the course of the iteration procedure the sum of squares of deviations of the calculated relaxation times from the experimental ones, weighted by reciprocals of the experimental errors of particular data, was minimized using

TABLE 5: Rotational Diffusion Parameters Found from the Relaxation Data Analysis for 9-(Trideuteromethyl)purine and 7-(Trideuteromethyl)purine in CD₃OD Solutions Assuming Anisotropic Reorientation of the Solute Molecules According to Rotational Diffusion Model of a Planar Top

sample	concn/M	α /deg	D_x^b	D_y^b	D_z^b	D_x/D_z	D_y/D_z
1a	1.30	5.9	1.77	1.06	0.67	2.63	1.58
1d	0.52	-0.4	1.85	1.03	0.73	2.54	1.41
1b	0.61	5.6	1.98	1.25	0.69	2.88	1.82
1c	0.13	12.7	2.39	1.43	0.95	2.52	1.51
2d	0.31	118.4	1.39	1.15	0.54	2.60	2.15
2b	0.56	115.7	1.50	1.30	0.53	2.83	2.45
2c	0.13	74.2	1.57	0.97	0.64	2.45	1.52

^a Angle between inertia (x_I) and diffusion (x_D) axes. ^b In 10^{10} s^{-1} .

the Newton–Raphson algorithm. The optimization was repeated starting from 16 different trial values of the angle α and various sets of diffusion coefficients. Generally, the result was almost insensitive to the starting values of the fitted parameters and only very few runs did not converge. For both compounds investigated almost all experimental data points were reproduced excellently (Tables 3 and 4). The results showed that only in the case of **2b** the line width of the broadest ¹⁴N signal was biased with an error of ca. 15%, as it was mentioned earlier. This experimental value was thus included into the fitting procedure with the appropriately diminished weight.

The uniqueness and credibility of the solution found was tested using a Monte Carlo simulation. Namely, 300 trial pseudoexperimental data sets were generated by adding random noise to the original experimental relaxation data. This noise had Gaussian distribution of the width equal to the error estimate, δ_i , of a given experimental data point. The amplitude of the noise was truncated by the limits $\pm 2\delta_i$. Then, the relaxation equations were solved for each trial data set and the result of this simulation was presented graphically in the form of a 3D picture for diffusion coefficients or as separate plots illustrating the distribution of the obtained α angle values. The illustrative examples of the results of such analysis for 9-methylpurine (sample **1a**) are given in Figure 3. The dispersion of points in these figures proves the uniqueness of the least-squares solution of the involved relaxation equations and estimates the uncertainty of the parameter values.

Interpretation of the Diffusion Parameters. The values of diffusion coefficients D_x , D_y , and D_z (the principal values of the diffusion tensors) and the angle α defining the orientation of the principal diffusion axes with respect to the axes of the inertia tensor, found for particular samples, were collected in Table 5 and shown in Figure 4. The examination of those values or appropriate ratios [D_x/D_z , $D_x(\mathbf{2d})/D_x(\mathbf{2b})$, $D_x(\mathbf{2c})/D_x(\mathbf{2b})$, etc., $s = x, y, z$] shows that $D_y(\mathbf{2c})$ is probably biased with an error, whereas all other results are internally consistent. Before discussion of those results, the labeling of the axes and the definition of the angle α require some comments. The symmetry of the investigated molecules ensures that one of the principal axes of the involved diffusion and inertia tensors is perpendicular to the aromatic ring plane. This axis was selected to be z -axis. For planar rotors this distinguished axis is connected with the highest moment of inertia. The labeling of the remaining axes was assumed to obey the relation $I_{yy} \geq I_{xx}$ between the principal moments of inertia or $D_y \leq D_x$ in the case of diffusion axes. It is necessary to assume additional convention concerning the sign of angle α . The positive sign of α denotes clockwise turning of the diffusion x -axis from the inertia x -axis in the Figure 4. When interpreting the results, it is important to realize that for both the inertia and diffusion axes their sense is not defined. Thus, α is equivalent to $(n \cdot 180 + \alpha)$ ($n = \text{integer number}$).

Examination of the results collected in Table 5 and especially the values of D_x/D_z ratio shows that reorientation of both

investigated molecules is highly anisotropic. The reorientation rate of **1** increases when its concentration decreases, whereas its tumbling anisotropy seems not to be affected by the concentration. This observation is attributable to the expected solution viscosity changes. In all investigated solutions of **1** the molecular reorientation is in full agreement with the inertia properties. Namely, the diffusion and inertia axes almost coincide (small α angles) and, simultaneously, the sequence of the diffusion coefficients is opposite to the sequence of the moments of inertia ($D_x > D_y > D_z$ and $I_{xx} < I_{yy} < I_{zz}$). In the solutions of comparable concentrations **2** reorients more slowly than **1** [cf. $D_x(\mathbf{1b})/D_x(\mathbf{2b})$, $D_x(\mathbf{1c})/D_x(\mathbf{2c})$, and $D_x(\mathbf{1d})/D_x(\mathbf{2d})$]. In the case of **2** the obtained results clearly show that in this case the directions of the diffusion axes definitely do not coincide with the inertia axes of a free nonsolvated molecule. It is interesting, however, that the directions of these diffusion axes roughly coincide with the inertia axes of the agglomerate composed of **2** molecule and two (or three) methanol molecules bonded to the former by hydrogen bonds to N-3 and N-9 (and N-1). Our experimental data do not allow definite statement that the lifetimes of hydrogen-bonded complexes are remarkably longer than the reorientation correlation time, but a consistent interpretation of our relaxation data requires assuming that the solvation of the investigated solutes in methanol is different. Somewhat imprecisely we can say that while the solvation of molecule of **1** is isotropic, the solvation of **2** is anisotropic. In this context it is worth noting that the calculated molecular dipole moment of **2** (8.78 D) is higher than that of **1** (5.66 D).

Conclusions

Reorientation of 9-(trideuteriomethyl)purine and 7-(trideuteriomethyl)purine molecules in methanol-*d*₄ solutions has been investigated on the basis of the interpretation of the nuclear spin relaxation rates of their ¹⁴N (or ¹H) and ¹³C nuclei. The molecular geometries, scalar coupling constants, and EFG tensors needed for the quantitative interpretation of these data have been calculated theoretically [DFT B3LYP/6-311++G-(2d,p) or B3PW91/6-311+G(df,pd)] with the inclusion of the impact of the solvent by using discrete solvation and polarizable continuum model. To get the fully consistent interpretation of the relaxation data, the effective C–H bond lengths being 3% longer than the calculated ones had to be used in the analysis to compensate for the ground-state vibrations. The reorientation of the investigated purines has been described as rotational diffusion of an asymmetrical top. It has been found that reorientation of both investigated molecules is highly anisotropic. The symmetry of the investigated molecules ensures that one of the principal axes of the involved diffusion and inertia tensors (z -axis) is perpendicular to the aromatic ring plane. This distinguished axis is connected with the highest moment of inertia and the slowest diffusion. For the remaining axes the relations $I_{yy} \geq I_{xx}$ between the principal moments of inertia and

$D_y \leq D_x$ in the case of diffusion axes are obeyed. In the case of **1** the diffusion and inertia axes almost coincide so that the molecular reorientation is in full agreement with the inertia properties. It is not the case for **2**, where the directions of the diffusion axes definitely do not coincide with the inertia axes of a free nonsolvated molecule. On the other hand, the directions of these diffusion axes roughly coincide with the inertia axes of the solvate composed of **2** and two (or three) methanol molecules. Moreover, in the solutions of comparable concentrations **1** reorients faster than **2**. Apparently, the mode of solvation of the investigated molecules is remarkably different, in spite of their structural similarity. This study confirms once again that careful interpretation of relaxation data can provide a lot of interesting and unique information concerning the behavior of molecules in solutions and their solvation.

Acknowledgment. This work was financially supported by Warsaw University of Technology.

Supporting Information Available: Calculated magnetic shielding tensors in the molecular axes frame of nuclei in 9-methylpurine complex with three methanol molecules and found optimum molecular geometries of both methylpurines solvated by methanol. This material is available free of charge via the Internet at <http://pubs.acs.org>.

References and Notes

- (1) Kowalewski, J. *Annu. Rep. NMR Spectrosc.* **1991**, 23, 289.
- (2) Dölle, A.; Bluhm, T. *Prog. Nucl. Magn. Reson. Spectrosc.* **1989**, 21, 175.
- (3) For example, see the following: Ludwig, R. In *Nuclear Magnetic Resonance*; Webb, G. A., Ed.; Specialist Periodical Reports; The Royal Society of Chemistry: London, 2004; Vol. 33, p 192 and references therein and in related chapters in earlier volumes.
- (4) Kumar, A.; Grace, R. C. R.; Madhu, P. K. *Prog. Nucl. Magn. Reson. Spectrosc.* **2000**, 37 (3), 191.
- (5) Palmer, A. G. *Annu. Rev. Biophys. Biomol. Struct.* **2001**, 30, 129.
- (6) Kempf, J. G.; Loria, J. P. *Cell Biochem. Biophys.* **2003**, 37 (3), 187.
- (7) Lucas, N. *Mol. Phys.* **1971**, 22, 147.
- (8) Sykora, S.; Vogt, J.; Bösigler, H.; Diehl, P. *J. Magn. Reson.* **1979**, 36, 53.
- (9) Henry, E. R.; Szabo, A. *J. Chem. Phys.* **1985**, 82, 4753.
- (10) McCain, D. C.; Markley, J. L. *J. Am. Chem. Soc.* **1986**, 108 (15), 4259.
- (11) Hardy, E. H.; Witt, R.; Dölle, A.; Zeidler, M. D. *J. Magn. Reson.* **1998**, 134 (2), 300.
- (12) Ejchart, A.; Zimniak, A.; Oszczapowicz, I.; Szatyłowicz, H. *Magn. Reson. Chem.* **1998**, 36 (8), 559.
- (13) Hardy, E. H.; Merkling, P. J.; Witt, R.; Dölle, A. *Z. Phys. Chem. (Muenchen)* **2000**, 214 (12), 1687.
- (14) Gryff-Keller, A.; Molchanov, S. *Magn. Reson. Chem.* **2000**, 38 (1), 17.
- (15) Kowalewski, J.; Effemey, M.; Jokisaari, J. *J. Magn. Reson.* **2002**, 157 (2), 171.
- (16) Wallach, D.; Huntress, W. T., Jr. *J. Chem. Phys.* **1969**, 50 (3), 1219.
- (17) Marchal, J. P.; Brondeau, J.; Canet, D. *Org. Magn. Reson.* **1982**, 19 (1), 1.
- (18) Eriksen, T.; Pedersen, E. J. *Mol. Phys.* **1984**, 53 (6), 1411.
- (19) Marchal, J. P.; Canet, D. *J. Chem. Soc., Faraday Trans. 2* **1982**, 78, 435.
- (20) Martin, N. H.; Issa, M. H.; McIntyre, R. A.; Rodriguez, A. A. *J. Phys. Chem. A* **2000**, 104 (48), 11278.
- (21) Walker, O.; Mutzenhardt, P.; Haloui, E.; Boubel, J. C.; Canet, D. *Mol. Phys.* **2002**, 100 (17), 2755.
- (22) Walker, O.; Mutzenhardt, P.; Tekely, P.; Canet, D. *J. Am. Chem. Soc.* **2002**, 124 (5), 865.
- (23) Walker, O.; Mutzenhardt, P.; Joly, J. P.; Canet, D. *Chem. Phys. Lett.* **2002**, 357 (1–2), 103.
- (24) Hughes, R. M.; Mutzenhardt, P.; Bartolotti, L.; Rodriguez, A. A. *J. Mol. Liq.* **2005**, 116 (3), 139.
- (25) Huntress, W. T., Jr. *J. Chem. Phys.* **1968**, 48, 3524.
- (26) Hubbard, P. S. *J. Chem. Phys.* **1970**, 52, 563.
- (27) Canet, D. *Concepts Magn. Reson.* **1998**, 10, 291.
- (28) Walker, O.; Varadan, R.; Fushman, D. *J. Magn. Reson.* **2004**, 168 (2), 336.
- (29) Werbelow, L. In *Nuclear Magnetic Resonance Probes of Molecular Dynamics*; Tycko, R., Ed.; Kluwer Academic: Dordrecht, The Netherlands, 1994; Chapter 5.
- (30) Batta, G.; Kover, K. E.; Gervay, J.; Hornyak, M.; Roberts, G. M. *J. Am. Chem. Soc.* **1997**, 119 (6), 1336.
- (31) Andrec, M.; Inman, K. G.; Weber, D. J.; Levy, R. M.; Montelione, G. T. *J. Magn. Reson.* **2000**, 146 (1), 66.
- (32) Dosset, P.; Hus, J. C.; Blackledge, M.; Marion, D. *J. Biomol. NMR* **2000**, 16 (1), 23.
- (33) Gonnella, N. C.; Roberts, J. D. *J. Am. Chem. Soc.* **1982**, 104, 3162.
- (34) Freeman, R.; Hill, H. D. W.; Kaptein, R. *J. Magn. Reson.* **1972**, 7, 327.
- (35) Kowalewski, J.; Ericson, A.; Vestin, R. *J. Magn. Reson.* **1978**, 31, 165.
- (36) Frisch, M. J.; et al. *Gaussian 03*, revision B.05; Gaussian, Inc.: Pittsburgh, PA, 2003.
- (37) (a) Kowalewski, J. *Annu. Rep. NMR Spectrosc.* **1991**, 22, 307. (b) McConnell, J. *The Theory of Nuclear Magnetic Relaxation in Liquids*; Cambridge University Press: Cambridge, U.K., 1987. (c) Abragam, A. *The Principles of Nuclear Magnetism*; Oxford University Press: London, 1989. (d) Spiess, H. W. *NMR* **1978**, 15, 55. (e) Wasylishen, R. E. In *NMR Spectroscopy Techniques*; Dybowski C., Lichter R. L., Eds.; Marcel Dekker Inc.: New York, 1987. (f) Kowalewski J.; Mäler L. *Nuclear Spin Relaxation in Liquids: Theory, Experiments, and Applications*; CRC Press/Taylor & Francis Group: Boca Raton, FL, 2006.
- (38) (a) Sinoti, A. L. L.; Politi, J. R. S.; Freitas, L. C. G. *J. Mol. Struct. THEOCHEM* **1996**, 366 (3), 249. (b) Woutersen, S.; Mu, Y.; Stock, G.; Hamm, P. *Chem. Phys.* **2001**, 266 (2–3), 137. (c) Zielkiewicz, J. *Phys. Chem. Chem. Phys.* **2003**, 5 (15), 3193.
- (39) Tomasi, J.; Mennucci, B.; Cammi, R. *Chem. Rev.* **2005**, 105 (8), 2999.
- (40) Bailey, W. C. *Chem. Phys.* **2000**, 252 (1–2), 57.
- (41) Mirzaei, M.; Hadipour, N. L. *J. Phys. Chem. A* **2006**, 110 (14), 4833.
- (42) Mlynarik, V. *Prog. Nucl. Magn. Reson. Spectrosc.* **1986**, 18, 277.